Scientific paper

Differences in Unfolding Energetics of CcdB Toxins From *V. fischeri* and *E. coli*

Andrej Mernik,[1] Uroš Andjelković,[2] Igor Drobnak[1] and Jurij Lah[1,*]

[1] *Faculty of Chemistry and Chemical Technology, University of Ljubljana, Aškerčeva c. 5, SI-1000 Ljubljana, Slovenia*

[2] *Institute for Chemistry, Technology and Metallurgy, Department of Chemistry, University of Belgrade, Studentski trg 12 – 16, 11000 Belgrade, Serbia*

* *Corresponding author: E-mail: jurij.lah@fkkt.uni-lj.si*

Received: 01-02-2012

Dedicated to Prof. Dr. Gorazd Vesnaver on the occasion of his 70th birthday

Abstract

Ccd system is a toxin-antitoxin module (operon) located on plasmids and chromosomes of bacteria. $CcdB_F$ encoded by *ccd* operon located on *Escherichia coli* plasmid F and $CcdB_{Vfi}$ encoded by *ccd* operon located on *Vibrio fischeri* chromosome are members of the CcdB family of toxins. Native CcdBs are dimers that bind to gyrase-DNA complexes and inhibit DNA transcription and replication. While thermodynamic stability and unfolding characteristics of the plasmidic $CcdB_F$ in denaturant solutions are reported in detail, the corresponding information on the chromosomal $CcdB_{Vfi}$ is rather scarce. Therefore, we studied urea-induced unfolding of $CcdB_{Vfi}$ at various temperatures and protein concentrations by circular dichroism spectroscopy. Global model analysis of spectroscopic data suggests that $CcdB_{Vfi}$ dimer unfolds to the corresponding monomeric components in a reversible two-state manner. Results reveal that at physiological temperatures $CcdB_{Vfi}$ exhibits lower thermodynamic stability compared to $CcdB_F$. At high urea concentrations $CcdB_{Vfi}$, similarly to $CcdB_F$, retains a significant amount of secondary structure. Differences in thermodynamic parameters of $CcdB_{Vfi}$ and $CcdB_F$ unfolding can reasonably be explained by the differences in their structural features.

Keywords: Toxin-antitoxin module, CcdB, CcdA, protein unfolding, thermodynamics

1. Introduction

Toxin-antitoxin (TA) modules are operons located on plasmids and chromosomes of bacteria and archea. The *ccd* operon is a TA module encoding the toxin CcdB and the antitoxin CcdA. C-terminal domain of CcdA is intrinsically disordered and vulnerable for proteolytic attack. In the absence of *ccd* operon expression, CcdA is degraded by proteases faster than CcdB and is thus unable to form CcdA:CcdB complexes. This leads to activation of the toxin CcdB which binds to its cellular target, DNA gyrase, and inhibits DNA transcription and replication. When *ccd* operon is expressed CcdB action is inhibited by the formation of the CcdA:CcdB complexes. *ccd* expression is auto-regulated on the level of transcription by binding of the multimeric CcdA:CcdB complex, with CcdA/CcdB molar ratio of about 1:1, to the promoter DNA.[1–3]

ccd operon located on plasmid F of *Escherichia coli* encodes $CcdB_F$ which has been studied in detail both in terms of structure and thermodynamic stability.[3–7] On the other hand, very little thermodynamic information is available on CcdBs encoded by bacterial chromosomes. An example of chromosomal CcdB is $CcdB_{Vfi}$ from the marine bacterium *Vibrio fischeri*, that shows 41% sequence similarity to $CcdB_F$. Both $CcdB_F$ and $CcdB_{Vfi}$ form dimers in the solid state as well as in solution.[5,7–9] The structures of $CcdB_{Vfi}$ and $CcdB_F$ dimers show similarity of the secondary and tertiary structure (Figure 1). Each $CcdB_F$ and $CcdB_{Vfi}$ monomer consist of a major N-terminal β-sheet, a few smaller β-sheets and a C-terminal α-helix. In contrast to $CcdB_{Vfi}$, $CcdB_F$ has a notable charge separation due to a large number of positively charged amino acids located on β-sheet and the more negatively charged helix,[5,8] which may cause differences in thermodynamic stability of $CcdB_{Vfi}$ and $CcdB_F$.

In this work an attempt was made to characterize urea-induced unfolding of $CcdB_{Vfi}$ by CD spectroscopy. The obtained thermodynamic parameters were compared to the known values reported for $CcdB_F$.[4,6] The observed differences in thermodynamic stability of $CcdB_{Vfi}$ and $CcdB_F$ are discussed in terms of structural differences between the two proteins.

2. Experimental

Proteins were prepared and purified as described elsewhere.[7,8] Solutions of $CcdB_{Vfi}$ were dialyzed against TRIS buffer (0.02 M TRIS, 0.15 M NaCl and 0.001 M EDTA with pH = 7.5). Their concentrations were determined by measuring the absorbance at 280 nm using the absorption coefficients calculated by the method introduced by Gill and von Hippel.[10] $CcdB_{Vfi}$ stock solutions were mixed with concentrated urea solutions to prepare solutions with final urea concentration ranging from 0 to 8 M.

Spectropolarimetry measurements were performed using the CD spectropolarimeter AVIV 62A DS (*Aviv Associates, Lakewood, NJ, USA*). Experimental conditions: (1) urea induced unfolding: temperature, T = 5 °C – 45 °C, wavelength, λ = 222 nm; (2) thermally induced unfolding: temperatures T = 20 °C – 85 °C, λ = 225 nm with step size 1 °C; (3) CD spectra: λ = 260 – 210 nm with step size 1 nm. Slit bandwidth was set to 2 nm. Temperature equilibration time was 2 minutes for thermally induced unfolding and 30 seconds for other measurements, signal averaging time was 10 seconds for thermally and urea induced unfolding and 3 seconds for other measurements. CD measurements were conducted for solutions with protein (monomer) concentration of about 3 μM (1 cm cuvette) and protein monomer concentration of about 30 μM (0.1 cm cuvette). The ellipticies, θ, measured at given wavelength corrected for the corresponding contribution of the buffer, were converted to molar ellipticies, $[\theta]$, by dividing with optical pathlength, l, in cm and protein concentration, c, in μM.

Protein structures needed for surface area calculations were derived from the PDB files 1X75 ($CcdB_F$) and 3KU8 ($CcdB_{Vfi}$). Solvent accessible surface areas (SASA) of native protein structures were estimated using the program Naccess 2.1.1.[11] SASA of for the unfolded proteins were calculated as the sum of accessibilities of the protein residues X located in the corresponding Ala-X-Ala tripeptides. SASA calculations were performed using the solvent probe size of 1.40 Å and Z-slices of 0.05 Å. Other parameters needed for SASA calculations were taken as the program default values.

3. Results and Discussion

3. 1. Thermally and Urea Induced Unfolding of $CcdB_{Vfi}$

Thermal denaturation monitored by CD spectroscopy reveals very high thermal stability of $CcdB_{Vfi}$. The

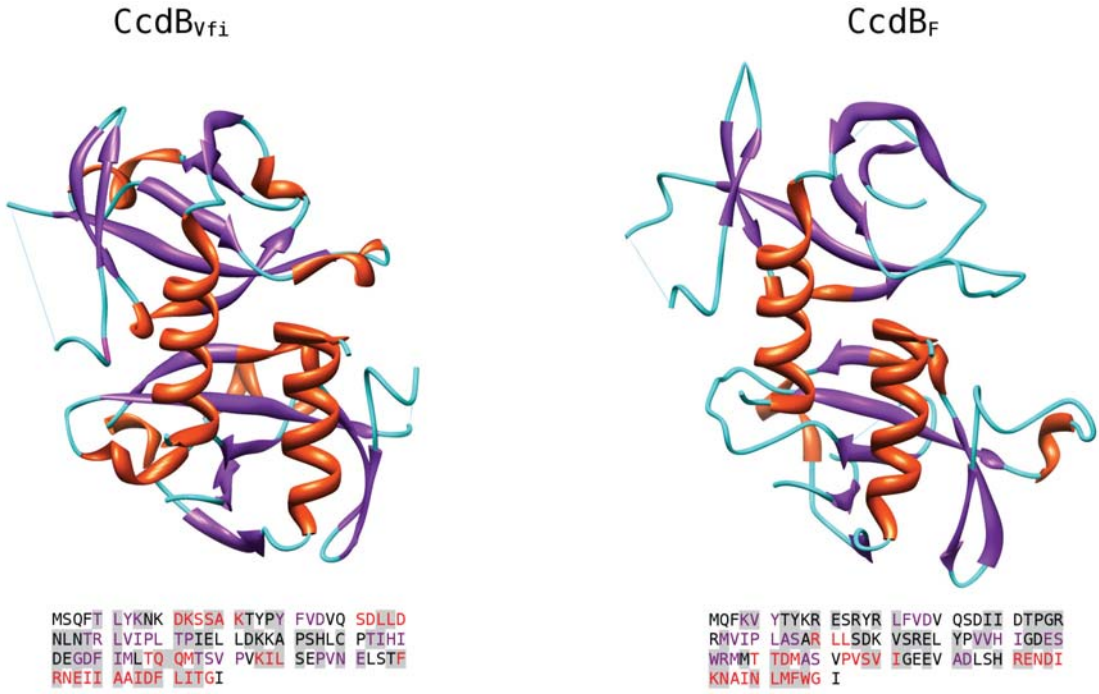

Figure 1: Comparison of crystal structures of $CcdB_{Vfi}$ and $CcdB_F$ dimers. Elements of secondary structure are colored red (α-helix) and violet (β-sheet). The structures were drawn with the program UCSF Chimera[15] from PDB files: 1X75 ($CcdB_F$) and 3KU8 ($CcdB_{Vfi}$). Gray marked regions that represent the difference in protein primary sequences (monomers) were obtained using the program SIM.[16]

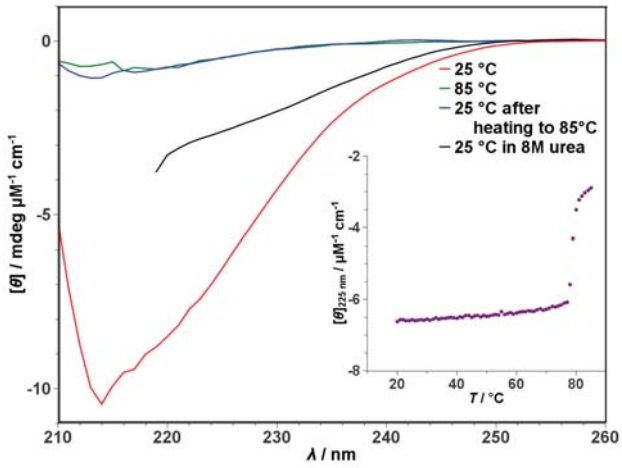

Figure 2: CD spectra and melting curve of $CcdB_{Vfi}$. Rescan at 25 °C was performed after cooling from 85 °C and 10 min incubation at 25 °C. CD spectrum measured in 8 M urea indicates significant fraction of residual secondary structure of $CcdB_{Vfi}$ in the urea denatured state. Inset: Thermal denaturation followed at 225 nm.

thermally induced denaturation transition is irreversible and occurs at temperatures above 70 °C (Figure 2). Denaturation was also induced by addition of denaturant urea and monitored by CD spectroscopy at various temperatures (Figures 3 and 4). To test the reversibility of the observed urea induced denaturation transition we prepared solutions with fixed protein and different urea concentrations by dilution of (denatured) protein solutions prepared in 8 M urea. Since the extent of recovery of ellipticity is very high (Figure 3) and independent on the protein concentration between 3 and 30 μM we considered the observed urea denaturation to be a reversible process.

3. 2. Urea Induced Unfolding of $CcdB_{Vfi}$ as Two-state Dimer-monomer Transition

Since $CcdB_{Vfi}$ exists as a (native) dimer in both, the solid state and in the solution,[8,9] we attempted to describe its urea induced unfolding as a reversible two-state process

$$N_2 \xleftrightarrow{K_{(T,u)}} 2D \tag{1}$$

where N_2 represents the native $CcdB_{Vfi}$ dimer, D the denatured $CcdB_{Vfi}$ monomer and $K_{(T,u)}$ the apparent equilibrium constant which is a function of temperature (T) and molar urea concentration (u). $K_{(T,u)}$ is defined as:

$$K_{(T,u)} = \frac{[D]^2}{[N_2]} = \frac{\alpha^2_{(T,u)}}{1-\alpha_{(T,u)}} 2c \tag{2}$$

where $[N_2]$ and [D] represent equilibrium molar concentrations of N_2 and D. In equation 2 $\alpha_{(T,u)}$ is the fraction of CcdB in the denatured state at given T and u defined as $\alpha_{(T,u)} = [D]/c$, where c is the total molar concentration of $CcdB_{Vfi}$ monomers. According to the suggested model (equation 1), the measured ellipticity at a given wavelength corrected for the corresponding buffer contribution normalized to c = 1 μM and l = 1 cm, $[\theta]_{(T,u)}$, can be expressed as:

$$[\theta]_{(T,u)} = (1-\alpha_{(T,u)})[\theta]_{N_2(T,u)} + \alpha_{(T,u)}[\theta]_{D(T,u)} \tag{3}$$

where $[\theta]_{N_2(T,u)}$ and $[\theta]_{D(T,u)}$ represent the corresponding molar ellipticities of N_2 and D given per mol of $CcdB_{Vfi}$ monomer that can be estimated at any measured T as linear functions of urea concentration u (pre- and post-transitional baselines presented in Figure 3). The measured $\alpha_{(T,u)}$ (Figure 4) can be expressed as:

$$\alpha_{(T,u)} = \frac{[\theta]_{(T,u)} - [\theta]_{N_2(T,u)}}{[\theta]_{D(T,u)} - [\theta]_{N_2(T,u)}} \tag{4}$$

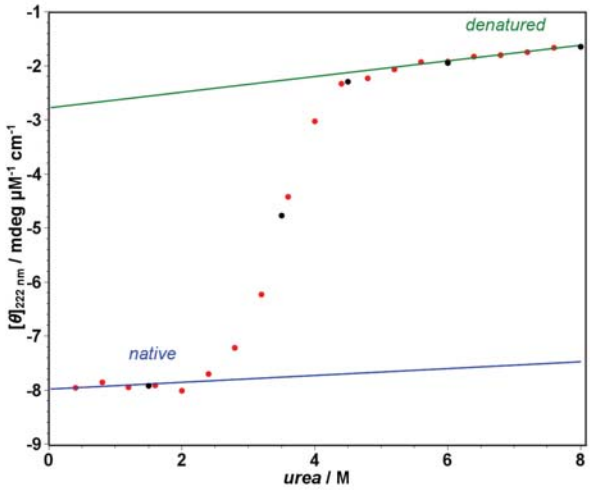

Figure 3: Typical urea-induced CD denaturation curve (red symbols) of $CcdB_{Vfi}$ (molar ellipticity, $[\theta]_{(T,u)}$, versus *urea* concentration) measured at c = 29.6 μM and 5 °C. Black symbols represent molar ellipticites measured for $CcdB_{Vfi}$ solutions obtained by dilution of $CcdB_{Vfi}$ solutions prepared in 8 M urea (reversibility test). Blue and green line represent the molar ellipticities $[\theta]_{N_2(T,u)}$ and $[\theta]_{D(T,u)}$ corresponding to the native and denatured state, respectively. Together with the measured molar ellipticies $[\theta]_{(T,u)}$ they were used in calculations of fractions of the protein in the denatured state $\alpha_{(T,u)}$ (equation 4).

On the other hand, $\alpha_{(T,u)}$ can be connected to the energetics of unfolding through the two-state transition model (equation 1). According to this model the dependence of the apparent standard Gibbs free energy of unfolding ($\Delta G^\circ_{(T,u)}$) on u can be at any T expressed as:

$$\Delta G^\circ_{(T,u)} = \Delta G^\circ_{(T)} - m \cdot u \tag{5}$$

where m is an empirical parameter strongly correlated to

the changes of protein accessible surface upon unfolding[12] and assumed to be temperature independent. $\Delta G^{\circ}_{(T)}$ is the standard Gibbs free energy of unfolding in the absence of urea ($u = 0$) that may be expressed in terms of the corresponding standard Gibbs free energy ($\Delta G^{\circ}_{(T_0)}$) and standard enthalpy of unfolding ($\Delta H^{\circ}_{(T_0)}$) at a reference temperature $T_o = 25$ °C and standard heat capacity of unfolding (ΔC°_P) (assumed to be temperature independent) through the Gibbs-Helmholtz relation (integrated form):

$$\Delta G^{\circ}_{(T)} = T\left\{\frac{\Delta G^{\circ}_{(T_o)}}{T_o} + \Delta H^{\circ}_{(T_o)}\left[\frac{1}{T} - \frac{1}{T_o}\right] + \Delta C^{\circ}_P\left[1 - \frac{T_o}{T} - \ln\frac{T}{T_o}\right]\right\} \quad (6)$$

It follows from equations 5 and 6 that the model (adjustable) thermodynamic parameters $\Delta G^{\circ}_{(T_0)}$, $\Delta H^{\circ}_{(T_0)}$, ΔC°_P and m define $\Delta G^{\circ}_{(T,u)}$ and also the corresponding $K_{(T,u)}$ ($K_{(T,u)} = \exp(-\Delta G^{\circ}_{(T,u)}/RT)$). Thus, the model function for $\alpha_{(T,u)}$ can be derived from equation 2 as:

$$\alpha_{(T,u)} = \sqrt{\left(\frac{K_{(T,u)}}{4c}\right)^2 + \frac{K_{(T,u)}}{2c}} - \frac{K_{(T,u)}}{4c} \quad (7)$$

its value at any T and u can be calculated for a given set of adjustable parameters and compared to $\alpha_{(T,u)}$ values estimated experimentally from equation 4. The values of adjustable parameters (Table 1) were obtained by global fitting of the model function (equation 7) to the family of CD unfolding curves measured at various temperatures (Figure 4) using the non-linear Levenberg–Marquardt regression procedure. Global fitting results in a good agreement between the model and experimental data. Moreover, unfolding curves measured at about ten times lower $CcdB_{Vfi}$ concentration (Figure 4-inset) show that unfolding at this concentration occurs at lower u suggesting that the transition is not monomolecular. In this light the observation that the model function (equation 7) is able to describe the curves measured at lower $CcdB_{Vfi}$ concentration well using the same set of adjustable parameters (Table 1), represents additional support of the proposed model of $CcdB_{Vfi}$ dimer denaturation accompanied by dissociation of subunits (equation 1). Therefore, and due to the observed good quality of the global fit we consider the obtained thermodynamic parameters to be reliable and physically sound.

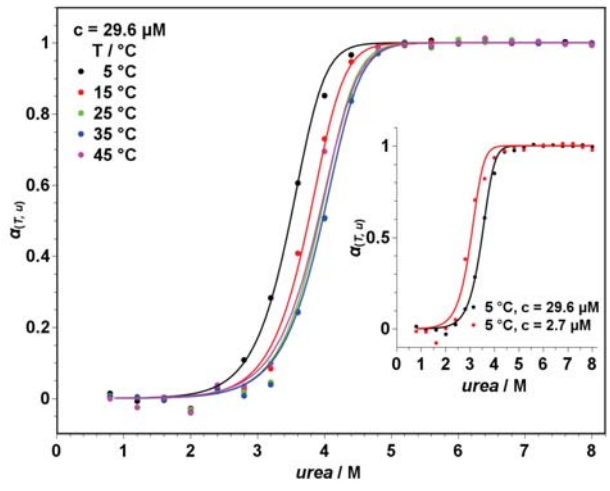

Figure 4: Global model analysis of urea induced denaturation od $CcdB_{Vfi}$. Fraction of the protein in the denatured state $\alpha_{(T,u)}$ as a function of *urea* concentration determined at various temperatures, T, and protein concentrations, c (inset). The points represent experimental data and the lines represent the best global fit of the model function (equation 7). The inset shows that the transition monitored at low c occurs at lower *urea* concentration and is well described by the corresponding model function based on the reversible two-state dimer-monomer model (equation 1).

3. 3. Differences in Unfolding Energetics Between $CcdB_{Vfi}$ and $CcdB_F$ and Their Structural Interpretation

Thermodynamic profile of $CcdB_{Vfi}$ unfolding (Figure 4) was obtained from the best global fit values of $\Delta G^{\circ}_{(T_0)}$, $\Delta H^{\circ}_{(T_0)}$, ΔC°_P (Table 1). They were used to estimate $\Delta G^{\circ}_{(T)}$ (from equation 6), $\Delta H^{\circ}_{(T)}$ from the Kirchhoff's law

$$\Delta H^{\circ}_{(T)} = \Delta H^{\circ}_{(T_o)} + \Delta C^{\circ}_P(T - T_o) \quad (8)$$

and the corresponding entropy contribution, $T\Delta S^{\circ}_{(T)}$, from the Gibbs relation

$$\Delta G^{\circ}_{(T)} = \Delta H^{\circ}_{(T)} - T\Delta S^{\circ}_{(T)} \quad (9)$$

Table 1: Comparison of the thermodynamic parameters of $CcdB_{Vfi}$ and $CcdB_F$ unfolding obtained from urea-induced denaturation studies.

	$CcdB_{Vfi}$	$CcdB_F$[a]	$CcdB_F - CcdB_{Vfi}$
$\Delta G^{\circ}_{(T_0)}$	18 ± 1	21 ± 1	3 ± 1
$\Delta H^{\circ}_{(T_0)}$	3 ± 1	25 ± 4	22 ± 4
$T_0\Delta S^{\circ}_{(T_0)}$	–15 ± 2	4 ± 5	19 ± 5
ΔC°_P	1.0 ± 0.2	2.6 ± 0.3	1.6 ± 0.4
m	3.0 ± 0.1	3 ± 3	0 ± 3

[a] Data taken from ref. 6.

A comparison of $\Delta G^{\circ}_{(T)}$ versus T curves (Figure 5a) for $CcdB_{Vfi}$ and $CcdB_F$ indicates that at physiological temperatures the thermodynamic stability of $CcdB_F$ is higher compared to $CcdB_{Vfi}$. On the other hand, the maximum stability for $CcdB_F$ is observed at lower temperature as for $CcdB_{Vfi}$. The obtained ΔC°_P of $CcdB_{Vfi}$ unfolding was compared to the corresponding ΔC°_P estimated as a function of no. of amino acid residues for a large set of proteins.[13] The comparison shows that the measured ΔC°_P represents only 42% of the value expected for the protein of the same size. This suggests that a degree of unfolding of $CcdB_{Vfi}$ in concentrated urea solutions is significantly lower than the degree of unfolding

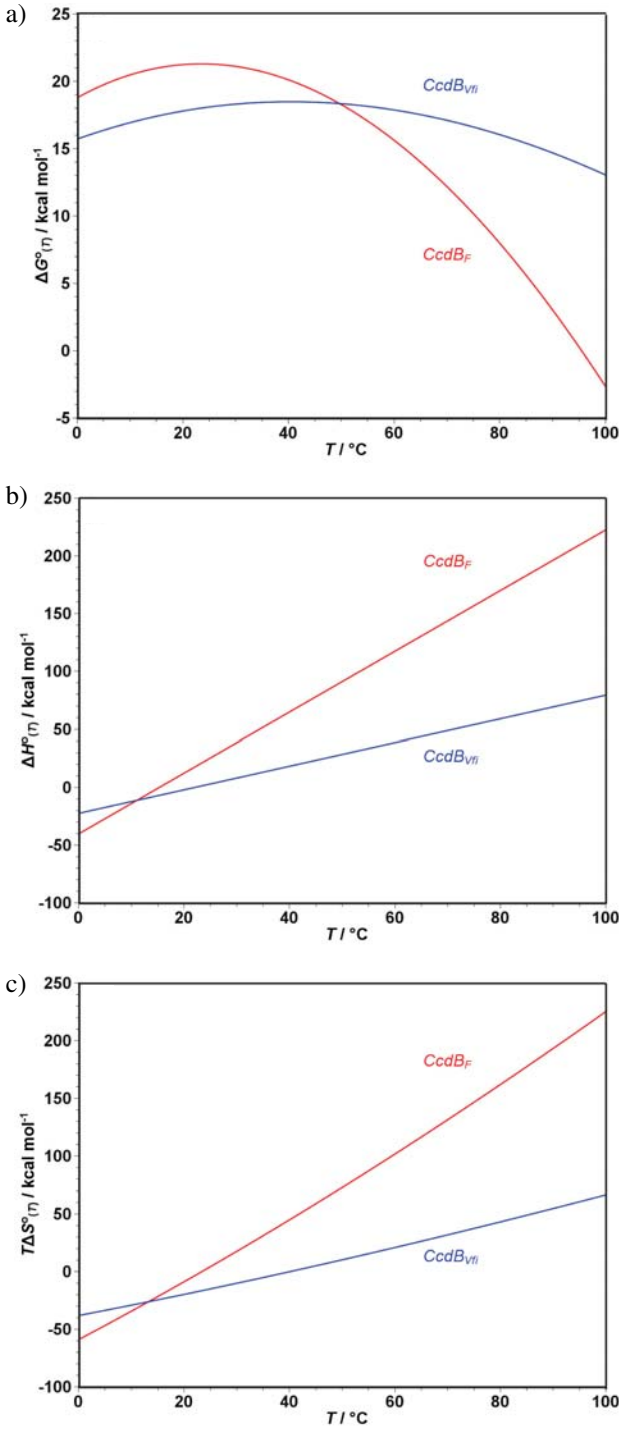

Figure 5. Thermodynamic profile of $CcdB_{Vfi}$ and $CcdB_F$ unfolding. (a) Standard Gibbs free energy, $\Delta G^\circ_{(T)}$; (b) enthalpy, $\Delta H^\circ_{(T)}$; (c) the corresponding entropy contribution, $T\Delta S^\circ_{(T)}$. All thermodynamic quantities extrapolated to urea concentration $u = 0$ are presented as functions of temperature. The profiles were calculated from the best-fit parameters (Table 1) by using equations 6, 8 and 9.

seen in an average protein of the large data set analyzed in ref. 13. The result is in accordance with those of the CD measurements (Figure 2) suggesting that $CcdB_{Vfi}$ in the urea denatured state retains a significant amount of secondary structure. Similar features of the urea unfolded state were observed also for previously studied $CcdB_F$.[6]

To correlate the observed differences in thermodynamic parameters of $CcdB_{Vfi}$ and $CcdB_F$ (Table 1, Figure 4), with differences in $CcdB_{Vfi}$ and $CcdB_F$ structural features structural characteristics of $CcdB_{Vfi}$ and $CcdB_F$ native (dimeric) and unfolded (monomeric) state are needed. One of those are solvent accessible surface areas (SASA). SASA of native $CcdB_{Vfi}$ and $CcdB_F$ were calculated from crystal structures presented in Figure 1. SASA of the unfolded proteins were approximated as the sum of SASA of the protein residues X located in the corresponding Ala-X-Ala tripeptides (the sum runs over all $CcdB_{Vfi}$ or $CcdB_F$ residues). The values are presented in Table 2.

Table 2: Solvent accessible surface areas (SASA) of $CcdB_{Vfi}$ and $CcdB_F$

	$CcdB_{Vfi}$	$CcdB_F$	$CcdB_F - CcdB_{Vfi}$
A_{polar} (2D) / 10³ Å^2	12.09	12.94	0.86
A_{polar} (N_2) / 10³ Å^2	3.69	3.81	0.12
ΔA_{polar} ($N_2 \rightarrow$ 2D) / 10³ Å^2	8.39	9.13	**0.74**
$A_{non\text{-}polar}$ (2D) / 10³ Å^2	19.33	18.99	–0.33
$A_{non\text{-}polar}$ (N_2) / 10³ Å^2	6.10	5.68	–0.42
A_{polar} ($N_2 \rightarrow$ 2D) / 10³ Å^2	13.23	13.31	**0.09**

It can be seen that the changes of polar SASA accompanying $CcdB_F$ unfolding are about 740 Å^2 higher than for $CcdB_{Vfi}$ unfolding. By contrast, the difference in changes of non-polar SASA of unfolding between $CcdB_F$ and $CcdB_{Vfi}$ is only about 90 Å^2. The empirical parameterizations correlating SASA of unfolding to the corresponding thermodynamic parameters[13,14] suggest that changes of polar SASA have much higher impact on $\Delta H^\circ_{(T)}$ while changes of non-polar SASA have much higher impact on ΔC°_P and $\Delta S^\circ_{(T)}$. Thus, the observed $\Delta\Delta H^\circ_{(T)} > 0$ and smaller magnitudes of $\Delta\Delta C^\circ_P$ and $T\Delta\Delta S^\circ_{(T)}$ resulting in $\Delta\Delta G^\circ_{(T)} > 0$ can be reasonably explained by differences in $CcdB_F$ and $CcdB_{Vfi}$ structural features.

4. Acknowledgment

We thank Prof. R. Loris for providing the purified toxin $CcdB_{Vfi}$ used in this work. Ministry of Higher Education, Science and Technology and Agency for Research of Republic of Slovenia are acknowledged for the financial support through the Grant No. P1-0201.

5. References

1. Buts, L., Lah, J., Dao-Thi, MH., Wyns, L., Loris, R., Toxin-antitoxin modules as bacterial metabolic stress managers, *Trends Biochem. Sci.*, **2005,** *30*, 672–679

2. Engelberg-Kulka, H., Glaser, G., Addiction Modules and Programmed Cell Death and Antideath in Bacterial Cultures, *Annu. Rev. Microbiol.*, **1999,** *53*, 43–70
3. De Jonge, N., Garcia-Pino, A., Buts, L., Haesaerts, S., Charlier, D., Zangger, K., Wyns, L., De Greve, H., Loris, R., Rejuvenation of CcdB-Poisoned Gyrase by an Intrinsically Disordered Protein Domain, *Mol. Cell*, **2009,** *35*, 154–163
4. Šimić, M., De Jonge, N., Loris, R., Vesnaver, G., Lah, J., Driving Forces of Gyrase Recognition by the Addiction Toxin CcdB, *J. Biol. Chem.,* **2009,** *284*, 20002–20010
5. Loris, R., Dao-Thi, MH., Bahassi, EM., Van Melderen, L., Poortmans, F., Liddington, R., Couturier, M., Wyns, L., Crystal Structure of CcdB, a Topoisomerase Poison from *E. coli*, *J. Mol. Biol.*, **1999,** *285*, 1667–1677
6. Šimić, M., Vesnaver, G., Lah, J., Thermodynamic Stability of the Dimeric Toxin CcdB, *Acta Chim. Slov.*, **2009,** *56*, 139–144
7. Dao-Thi, MH., Wyns, L., Poortmans, F., Bahassi, EM., Couturier, M., Loris, R., Crystallization of CcdB, *Acta Crystallogr.*, **1998,** *D54*, 975–981
8. De Jonge, N., Hohlweg, W., Garcia-Pino, A., Respondek, M., Buts, L., Haesaerts, S., Lah, J., Zangger, K., Loris, R., Structural and thermodynamic characterization of *Vibrio fischeri* CcdB, *J. Biol. Chem.*, **2010,** *285*, 5606–5613
9. De Jonge, N., Buts, L., Vangelooven, J., Mine, N., Van Melderen, L., Wyns, L., Loris, R., **2007,** Purification and crystallization of *Vibrio fischeri* CcdB and its complexes with fragments of Gyrase and CcdA, *Acta Crystallogr.*, *F63*, 356–360
10. Pace, C. N., Vajdos, F., Fee, L., Grimsley, G., Gray, T., How to measure and predict the molar absorption coefficient of a protein, *Protein Sci.,* **1995,** *4*, 2411–2423
11. Hubbard, S. J., Thornton, J. M., 'NACCESS', Computer Program, *Department of Biochemistry and Molecular Biology, University College London* **1993.**
12. Myers, JK., Pace, CN., Scholtz, JM., Denaturant *m* values and heat capacity changes: Relation to changes in accessible surface areas of protein unfolding, *Protein Sci.,* **1995,** *4*, 2138–2148
13. Robertson, AD., Murphy, KP., Protein Structure and the Energetics of Protein Stability, *Chem. Rev.,* **1997,** *97*, 1251–1267
14. Murphy, KP., Freire, E., Thermodynamics of structural stability and cooperative folding behavior in proteins, *Adv. Protein Chem.,* **1992,** *43*, 313–361
15. Pettersen EF., Goddard TD., Huang CC., Couch GS., Greenblatt DM., Meng EC., Ferrin TE., UCSF Chimera – a visualization system for exploratory research and analysis, *J. Comput. Chem.*, **2004,** *25*, 1605–1612
16. Huang, XQ., Miller, W., A Time-Efficient, Linear-Space Local Similarity Algorithm, *Adv. Appl. Math.,* **1991,** *12*, 337–357

Povzetek

Genetski sistem *ccd* je predstavnik t.i. modulov toksin-antitoksin, ki se nahajajo na plazmidih in kromosomih različnih bakterij. $CcdB_F$, katerega genetski zapis je vsebovan na plazmidu F *Escherichie coli* in $CcdB_{Vfi}$, katerega genetski zapis je vsebovan na kromosomu *Vibrio fischeri*, pripadata družini toksinov CcdB. Nativna proteina $CcdB_F$ in $CcdB_{Vfi}$ sta dimera, ki se vežeta na kompleks giraze z DNA in tako inhibirata prepisovanje in podvojevanje DNA. Medtem ko so termodinamska stabilnost in značilnosti razvitja plazmidnega $CcdB_F$ v raztopinah denaturantov dobro poznane, so informacije o omenjenih značilnostih $CcdB_{Vfi}$ zelo redke. Zato smo s spektropolarimetrijo proučevali razvitje $CcdB_{Vfi}$ v raztopinah sečnine pri različnih temperaturah. Globalna modelska analiza spektroskopskih podatkov pokaže, da je denaturacija enostopenjski prehod, pri katerem se dimer $CcdB_{Vfi}$ razvije in hkrati disociira v dva monomera. Rezultati kažejo, da ima pri fizioloških temperaturah $CcdB_{Vfi}$ nižjo termodinamsko stabilnost od $CcdB_F$. Podobno kot $CcdB_F$ pa pri visokih koncentracijah sečnine ohrani znatno količino sekundarne strukture. Razlike v termodinamskih parametrih razvitja $CcdB_{Vfi}$ and $CcdB_F$ je mogoče smiselno pojasniti z razlikami v njunih strukturnih značilnostih.